Unmanned Systems, Vol. 14, No. 2 (2026) 307–321

DOI: 10.1142/S2301385026500019

UNMANNED SYSTEMS
https://www.worldscientific.com/worldscinet/us

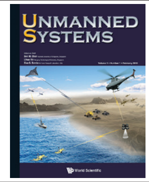

Distributed Unmanned Vehicle Platoon Control: A Combining Intention Recognition Method

Yige Ren [*], Kang Song [†,¶], Jin Guo [*,‡], Yanlong Zhao [§]

[*] *School of Automation and Electrical Engineering, University of Science and Technology Beijing, Beijing 100083, P. R. China*

[†] *State Key Laboratory of Engines, School of Mechanical Engineering, Tianjin University, Tianjin 300072, P. R. China*

[‡] *Key Laboratory of Knowledge Automation for Industrial Processes, Ministry of Education, Beijing 100083, P. R. China*

[§] *Key Laboratory of Systems and Control, Institute of Systems Science, Academy of Mathematics and Systems Science, Chinese Academy of Sciences, Beijing 100190, P. R. China*

This paper aims to improve the safety of road traffic and design a vehicle platoon controller based on the vehicle lane-changing intention recognition model. Through deep learning technology, the lane-changing intention of surrounding vehicles on the road is detected in real-time. First, we used the Generative Adversarial Networks (GAN) network to increase the number of lane-changing data in the original data, and train a deep neural network model based on the Long Short-Term Memory (LSTM) network, with the model accuracy reaching 93.54%. Based on the intent recognition model, the leading vehicle adjusts the longitudinal distance from the surrounding vehicles according to the probability of the detected intent to change lanes, to ensure the safety of the platoon during the lane-changing process of the surrounding vehicles. Finally, the related simulation verification is carried out by Matlab/Simulink joint Prescan, and the experimental results show that the proposed method recognizes a difference of 0.4 s between the time of generating lane change intention and the actual time.

Keywords: Lane change intention recognition; LSTM; GAN; sliding mode control; vehicle platoon.

1. Introduction

In recent years, the number of motor vehicles in China has increased dramatically, and the National Bureau of Statistics predicts that by 2022, the number of civilian vehicles will reach 311.8444 million, and the number of drivers will increase to 464.3441 million, so road traffic safety will be challenged. Meanwhile, Unmanned autonomous vehicle (UAV) technology is developing rapidly, with a 2005 report proposing "fully autonomous swarms" as a high-level goal for UAV control [1]. Accurate recognition of the intent of surrounding vehicles in intelligent driving systems has become particularly critical, which not only provides more reaction time for decision-making control of vehicles, but also effectively improves driving safety.

In addition, vehicle platoon technology also has important social and economic values in terms of reducing the labor intensity of drivers, improving the safety of platoon driving, and reducing fuel consumption by shortening the

Received 1 July 2024; Revised 16 December 2024; Accepted 17 December 2024; Published 18 March 2025. This paper was recommended for publication in its revised form by editorial board member, Feng Lin.
Email Address: ¶*songkangtju@tju.edu.cn*
¶Corresponding author.

distance between vehicles. Global experimental projects such as the PATH project in the United States, the SARTRE project in Europe, and the EnergyITS truck platoon project in Japan are promoting the continuous innovation and development of vehicle platoon technology, and laying a solid foundation for the realization of a global intelligent transportation system [2].

With the rapid development of Intelligent Transportation Systems, accurately predicting drivers' driving intentions has become a critical task to ensure road safety. However, existing methods for lane change intention recognition and prediction still face many challenges in practical applications, which are mainly related to the accuracy, timeliness, and adaptability to the driving environment of prediction. Work [3] utilizes Hidden Markov Models to analyze the motion parameters of the car and driver, as well as the driver's eye gaze sequences, to achieve the prediction of the driver's lane change intention. Work [4] models and analyzes driver behavior based on structural pattern recognition methods with context-free and context-sensitive grammars, but the recognition accuracy of such methods is relatively low. To solve this problem, many studies have applied LSTM to the field of intent recognition [5]. The advantage of LSTM's ability to process temporal data makes it excellent in predicting lane change intent. For example, work [6] used an LSTM model to predict a driver's intention to turn in a complex intersection scenario, showing excellent accuracy and consistency. In addition, work [7] uses LSTM for lane change intention recognition in low-speed driving scenarios and combines it with the Light Gradient Booster Machine algorithm for risk prediction, which further enhances the utility of the model.

The work [8] further improves the accuracy of lane change intention recognition by combining the Attention Mechanism with the Temporal Convolutional Network. This combination not only improves the classification accuracy but also optimizes the prediction of multiple driving states in a multi-task learning framework. The application of such methods in multi-vehicle interaction scenarios, especially combining driving style and vehicle-vehicle interaction information, significantly improves the recognition rate of the model [9]. However, existing methods are still insufficient in dealing with the effects of complex external environments. Work [10] proposed a Hidden Markov Model-based lane change intention recognition method by introducing external environment decision factors and combining vehicle dynamic parameters and external environment factors, thus improving the recognition accuracy. In addition, work [11] also demonstrated the possibility of further improving the accuracy of lane change intention recognition by collecting multi-modal data in real-time and using a bidirectional long short-term memory network (BiLSTM) in a driving scenario in a connected environment.

Although existing studies have made some progress in lane change intention recognition, there are still some limitations, such as insufficient adaptability to complex external environments and lack of consideration for the amount of lane change data. Therefore, LSTM-based vehicle lane change intention recognition still needs to be further optimized, especially in terms of improving recognition accuracy and practicality in small sample situations.

With the advancement of autonomous driving and communication technologies, queuing of automated vehicles (AVs) has attracted much attention due to its potential to significantly improve traffic efficiency, and many state-of-the-art control algorithms and strategies have been proposed to cope with the queuing problem in complex traffic environments. For example, fuzzy theory [12], adaptive control [13], reinforcement learning [14], and differential games [15] can cope with uncertainty or traffic oscillations in the platooning system better, but still have deficiencies in coordinated control among different vehicles. Model predictive control (MPC) has been widely used in vehicle platoon control due to its advantages in dealing with system dynamics and constraints. To solve the distributed control problem in heterogeneous vehicle formations, work [16] proposed a distributed observer-based formation tracking control algorithm, which estimates the target state and achieves formation control through the information of neighboring nodes. Work [17] realized fuel-efficient control of heavy-duty vehicle formations through a two-tier control architecture, but this approach relies on complex preview information and requires further validation in real-world environments. Work [18] employed distributed backward horizon control algorithms to ensure asymptotic stability of the formation under nonlinear dynamics. However, the effectiveness of these algorithms depends on specific conditions and may have limitations in practical applications.

The Distributed Model Predictive Control (DMPC) algorithm is used for heterogeneous vehicle formation control to solve the problem of unknown desired setpoints in unidirectional topology [19]. The method ensures asymptotic stability and good tracking of the formation through local open-loop optimal control. Work [20] used MPC for longitudinal and lateral control of vehicles in complex traffic scenarios. Work [21] proposed a spatiotemporal safe corridor-based motion optimization framework that is capable of planning safe trajectories for multiple vehicles in dynamic obstacle environments. However, the MPC method has high computational complexity and relatively poor real-time performance, which makes it difficult to maintain stability and accuracy in highly dynamic and changing traffic environments. To address this problem, the work [22] proposed the coupled multi-objective iterative distributed model predictive control method, which aims to improve real-time tracking accuracy by optimizing the control strategy. However, the stability of MPC also depends on the reliability of the communication topology, which makes it show some vulnerability in the face of communication failures. Work [23, 24] combines PID and MPC methods to achieve longitudinal control without relying on a fixed physical model, and experimentally verifies that the framework can drive convoys safely and efficiently in complex traffic environments, but communication delays have the same impact on formation stability. For this reason, work [25] proposes Dynamic Information Flow Topology combined with DMPC to cope with communication disruptions in real-world environments. In addition, work [26] proposes different topology models to ensure the internal and serial stability of the formation system. Work [27] achieves optimization of controller gain in the presence of time-varying delays by combining the Routh–Hurwitz stability theorem and the Lyapunov–Razumikhin theorem. However, these methods tend to ignore the uncertainty of information transfer in real transportation environments, leading to limitations in the applicability of control strategies in practical applications.

Existing platoon control algorithms focus on improving the robustness, computational efficiency, and practicality of the algorithms to meet the demands in real transportation systems, and progress has been made in coping with complex control problems in self-driving vehicles. However, these methods still face challenges such as high computational complexity, high dependence on system initial conditions and topology, and insufficient adaptability in heterogeneous systems. Although LSTM-based deep learning models perform well on high-precision trajectory data, they are not robust enough in complex driving scenarios to adapt to the changing traffic environment and driver behavior on real roads. With the development of machine learning technology, how to realize the adaptation to the dynamically changing environment and the use of machine learning technology to perceive the environment will also become a key direction of research.

The introduction of LSTM has provided new paths for intent recognition and especially demonstrated significant advantages in handling time-series data. LSTM has shown excellent accuracy and utility in predicting driver steering intentions and incorporating risk prediction algorithms. However, even after the introduction of new methods such as attention mechanisms and spatio-temporal convolutional networks, existing techniques are still inadequate in dealing with the effects of complex external environments. In vehicle lane-changing intention recognition, the input of the network is temporal data, and researchers mostly use LSTM and its improved network for intention recognition by improving the model to increase prediction accuracy. However, due to different road parameters, road widths, and different driving habits of drivers, the accuracy of the model obtained from a single dataset trained in different scenarios will be affected to some extent. We improve the model accuracy by generative adversarial network expansion, which can get higher model accuracy in the situation of less data and can improve the adaptability of the model. In vehicle platoon control, autonomous vehicles have attracted much attention for their potential to improve transportation efficiency. Although methods such as fuzzy theory, adaptive control, and reinforcement learning have made progress in coping with uncertainty in platooning systems, and MPC has been widely used in vehicle platoon control due to its advantages in dealing with system dynamics and constraints, its real-time and computational complexity are still problems to be solved in highly dynamic environments. Compared to existing vehicle control methods, vehicles can track a reference trajectory over a while domain. The control method based on the deep learning algorithm we studied is different from the existing control methods, the vehicle needs to decide the control at the current moment according to the output of the deep learning algorithm. Unlike the existing methods, this paper considers more about how to realize the combination of deep learning algorithms and control methods from the application point of view. The specific system block diagram of this paper is shown in Fig. 1.

To address the shortcomings of existing technologies, this paper combines the TimeGAN with the designed LSTM intent recognition network to train a vehicle intent recognition model. This is aimed at resolving the robustness issues of current models in complex driving scenarios. Additionally, based on real-time detection results from the intent recognition model, a longitudinal controller for the platoon is designed to enhance the system's adaptability in real-world scenarios. Simultaneously, utilizing the status of the leading vehicle to control the remaining vehicles in the platoon enables the collective avoidance of surrounding vehicles, addressing the platoon control challenges in urban traffic. Our contribution is threefold and summarized as follows:

(i) Based on GAN-LSTM, a vehicle lane change intention recognition model is established, which enhances the intention recognition ability of the surrounding vehicles in the case of small samples.
(ii) Combining the intention recognition model with the vehicle controller increases the reaction time of the vehicle to external influences and improves safety.
(iii) Applied the information of the leading vehicle to the vehicle formation control to improve the safety of the platoon in the case of lane changing of the surrounding vehicles.

The remainder of this paper is organized as follows. Section 2 introduces the researched issues. Section 3

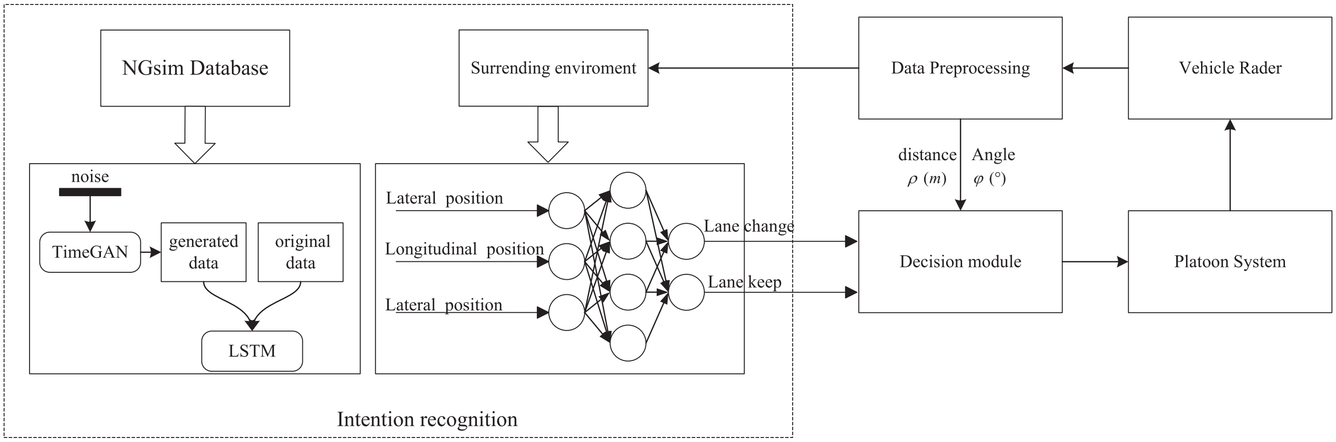

Fig. 1. System framework diagram.

introduces LSTM and GAN networks. A vehicle lane-changing intention recognition network is designed based on these two networks. Section 4 introduces the vehicle model and platoon controller, and designs the obstacle avoidance controller of the lead vehicle based on the intention recognition model obtained in Sec. 3. Section 5 gives the results of the intent recognition model trained in the python environment, and uses Matlab/Simulink combined with Prescan to build a vehicle simulation scene and conduct control simulation experiments. Section 6 summarizes the work.

2. Problem Description

In this paper, we consider the platoon of vehicles on a high-speed road under normal driving conditions and the presence of other vehicles around the front of the head vehicle, the surrounding vehicles will be switched into this lane at a certain moment, the specific scenario is shown in Fig. 2.

For this situation, the traditional method is to control based on the distance between the vehicles. However, the distance-based method has certain limitations. It leaves less reaction time for the leading car and even the platoon, and requires higher accuracy of the sensor. This paper is based on the intention recognition method and combines the historical trajectory data of surrounding vehicles with a deep learning algorithm to detect the lane-changing intention of the vehicle in the early stage of lane-changing and implement corresponding control according to different intentions. However, the amount of lane-changing data in the NGSIM dataset is much less than the amount of lane-keeping data. To ensure data balance and network accuracy, a generative adversarial network is used to expand the original data. To elucidate the problem studied in this paper and to simplify its complexity, a linear two-degree-of-freedom model of each vehicle in the platoon and of the surrounding vehicles in the environment is considered:

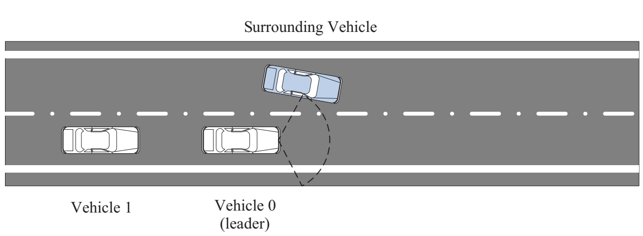

Fig. 2. Problem scenario schematic.

$$\dot{x}_i(t) = Ax_i(t) + Bu_i(t), \tag{1}$$

where $A = \begin{bmatrix} 0 & 1 & 0 \\ 0 & 0 & 1 \\ 0 & 0 & -\dfrac{1}{\tau_i} \end{bmatrix}$, $B = \begin{bmatrix} 0 \\ 0 \\ \dfrac{1}{\tau_i m_i} \end{bmatrix}$.

The leading car in the platoon uses millimeter wave radar to collect historical trajectory information of surrounding vehicles. The historical trajectory information of surrounding vehicles is represented by X:

$$X = [X_{i-l}, X_{i-l+1}, \ldots, X_{i-1}, X_i], \tag{2}$$

where $X_i = [x_i, y_i, v_{i,y}]$ represents the actual abscissa position of the surrounding vehicles obtained by converting the surrounding vehicle information received by the millimeter wave radar at time i. The vertical coordinate position, and the longitudinal speed, l is a positive integer, which is the length of the historical trajectory of the surrounding vehicles. The input l to the matching model is 20 time steps in length.

When it is detected that the surrounding vehicles have the intention to switch in, the longitudinal distance between the surrounding vehicles and the leading vehicle is $\Delta_x = x_s - x_0$, where x_s denotes the longitudinal position of the surrounding vehicles and x_0 denotes the longitudinal position of the leading vehicle. The leading vehicle maintains a safety distance $\Delta_s = 10(\mathrm{m})$ from the switching vehicle. According to the intention recognition probability, different weights γ are attached to the safety distance Δ_{env}. When $0.5 < P_I < 0.7$, the probability of changing lanes is not high, and the safety requirements are relatively relaxed. The weight value is $\gamma = 0.7$; When $0.7 < P_I < 0.9$, the probability of changing lanes increases. To ensure safety, the distance between the vehicle and the surrounding area is increased, with a weight value of $\gamma = 0.85$; when $0.9 < P_I$, it is assumed that surrounding vehicles will change lanes, maintain a safe distance, and take a weight value of $\gamma = 1$.

For the lead vehicle in the platoon, the control objective is $\lim_{t\to\infty}\|e_s\| = 0$. For the other vehicles in the platoon, take the safe distance $\Delta_i = l_i + q_i v_i + r_i a_i^2$, where $l_i = 10(\mathrm{m})$, q and r are positive real numbers. The control objective for the other vehicles is $\lim_{t\to\infty}\|e_i\| = 0$.

This paper primarily explores the integration of deep learning with vehicle platooning, focusing on the control problem of incorporating surrounding vehicle intent recognition in the context of longitudinal obstacle avoidance for the lead vehicle in a platoon. This paper begins by preprocessing the original NGSIM data through trajectory completion, filtering, and other techniques. To address the issue of imbalanced left and right lane-change data in the dataset, a GAN network is introduced to augment the small-sample data, aiming to enhance the model accuracy. An LSTM network is then designed to train the lane-change intent recognition model. Leveraging the intent recognition model, a sliding mode control method is employed to design the platoon's longitudinal controller and the lead vehicle's longitudinal obstacle avoidance controller. Finally, simulation experiments are conducted for numerical validation.

3. Vehicle Lane Change Intention Recognition

In the process of platoon travel, maintaining the overall control integrity of the vehicles often involves avoiding the insertion of other vehicles between the platoon. Therefore, in the practical scenario considered in this paper, the lead vehicle takes into account the information about surrounding vehicles both in front and to the left and right relative to the vehicle's heading, while other vehicles in the platoon consider how to maintain the stability of the platoon. In this scenario, the lead vehicle perceives the relative positions of surrounding vehicles, collects historical trajectory information of nearby vehicles, and the recognition model identifies their lane-change intentions based on this historical trajectory information.

Traditional methods such as support vector machines and random forests tend to output the average value of different intentions when the intentions of surrounding vehicles are unclear, making them less suitable for the scenario considered in this paper. In contrast, deep learning methods can accurately output probability values for different trajectory sequences, which is beneficial for controller design. This paper uses the publicly available NGSIM I-80 and NGSIM US-101 datasets as the original data and employs a GAN network to augment the original data, thereby increasing the diversity of the training dataset samples. Finally, an intent recognition network is designed based on LSTM, and the augmented dataset is used to train the intent recognition model.

3.1. *GAN algorithm*

The concept of the GAN was originally introduced by Goodfellow *et al.* [28]. Comprising two integral components, a generator network and a discriminator network, this architecture facilitates a dynamic interplay. The primary objective of the generator network is to synthesize target data from a predetermined distribution, while the discriminator network is tasked with discerning between original and generated data. The former endeavors to learn the generation of data that closely emulates real-world data, thereby challenging the discriminator's proficiency in identification. Conversely, the latter seeks to accurately discriminate whether the input originates from real or generated data. Through numerous cycles of adversarial training, the generator network progressively evolves to produce data closely mirroring real-world datasets. The GAN structure is shown in Fig. 3.

To enhance the generative capabilities for time series data, TimeGAN takes into account the inherent temporal correlations in time series data, combining the flexibility of unsupervised and supervised training [29]. By jointly optimizing supervised and adversarial objectives, the network can maintain the dynamics of training data during the sampling process, resulting in a significant improvement in generating realistic time series compared to baseline tests.

The generation process of TimeGAN combines open-loop and closed-loop modes, enabling the network to learn to

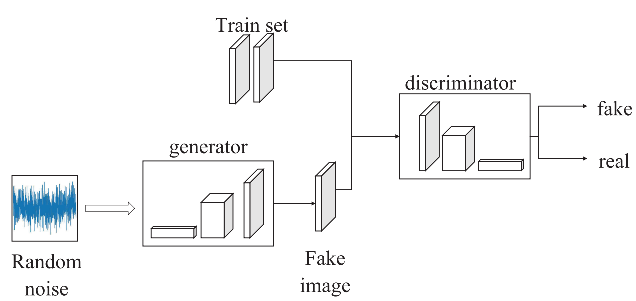

Fig. 3. GAN structure diagram.

capture dynamic features and temporal correlations in time series data. This combination enhances the network's ability to fit the distribution of real data, thus generating more realistic and temporally structured synthetic time series data.

Prior to the start of training, the training data were converted to 20×3 size and normalized mapping was performed. The network weights were initialized using a normal distribution with a standard deviation of 1.0 and the bias was initialized to zero. During training, the Adam optimizer was used and the learning rate was set to 0.001, and the network reconstruction loss, unsupervised loss, and supervised loss were

$$\begin{aligned} L_R &= E_{s,x_{1:T}}\left[\|s-\tilde{s}\|_2 + \sum_t \|x_t - \tilde{x}_t\|_2\right], \\ L_U &= E_{s,x_{1:T}}\left[\log y_S + \sum_t \log y_t\right] \\ &\quad + E_{s,x_{1:T}}\left[\log(1-\hat{y}_S) + \sum_t \log(1-\hat{y}_t)\right], \\ L_S &= E_{s,x_{1:T}}\left[\sum_t \|h_t - g_X(h_S, h_{t-1}, z_t)\|_2\right], \end{aligned} \tag{3}$$

where $s, x_{1:T}$ represents the original data sequence, s represents the static features, $x_{1:T}$ represents the time series features, T is the time series length, and $\hat{s}, \hat{x}_{1:T}$ represents the reconstructed data sequence. $y_S, y_{1:T}$ represents the identification result of the real data, $\hat{y}_S, \hat{y}_{1:T}$ represents the identification result of the generated data. $h_S, h_{1:T}$ denotes the potential representation of the original data and $\hat{h}_S, \hat{h}_{1:T}$ denotes the potential representation of the generated data. g_X is part of the generative network for generating the potential representation, and z_t is a random noise vector used as input to the generator network. By minimizing the three loss functions to optimize the network parameters, TimeGAN can generate generative data close to the original data distribution for training the recognition algorithm in the following section.

3.2. *Vehicle lane-changing intention recognition algorithm*

The inherent neural networks encounter difficulties in adeptly extracting temporal features from input data, notably in domains such as natural language processing and time series analysis. To overcome these challenges, Recurrent Neural Network incorporates a hidden layer concept, establishing connections between input time series and enabling the effective extraction of temporal features. Furthermore, LSTM networks, a specialized variant of recurrent neural networks, employ "gate" mechanisms to intricately capture long-term dependencies.

The model proposed in this paper is a deep learning structure combining Convolutional Neural Network and LSTM, designed to efficiently extract features from input sequence data and perform classification. The initial part of the model consists of multiple 1×1 convolutional layers using 64 and 128 convolutional kernels, and the learning capability and stability of the network are enhanced by Batch Normalization and ReLU activation functions after each convolutional layer. Residual connections are introduced between each set of convolutional layers to mitigate the gradient vanishing problem in deep network training and to improve the accuracy and efficiency of feature extraction. After feature extraction is completed, the model introduces a layer of the LSTM network, which is constructed with 128 units and outputs the complete sequence data. Besides, the generalization ability of the model is further improved by batch normalization and Dropout operation. After the Global Average Pooling Layer and the Dense Layer, the model outputs the triple classification results after the softmax activation function. The model structure is shown in Fig. 4.

The network achieves an organic integration of convolutional layers, residual connections, and recurrent layers, aiming to effectively capture local and temporal patterns in time series data. The initial convolutional block robustly captures local features of the input time series through a series of convolutional operations and batch normalization. The introduction of residual connections facilitates smooth information transfer, mitigating the vanishing gradient problem and enhancing the model's ability to model long-term dependencies. The subsequent recurrent layer adopts the LSTM structure, allowing the model to learn temporal dependencies in time series. Finally, global average pooling and a dense softmax layer are employed to obtain a fixed-length temporal feature representation and perform the ultimate classification.

The model in this paper is dependent on data distribution, and the data distribution during model training cannot fully cover the diversity in real roads, especially for roads with large changes in width and number of lanes or trajectory data under specific traffic scenarios (e.g. congestion,

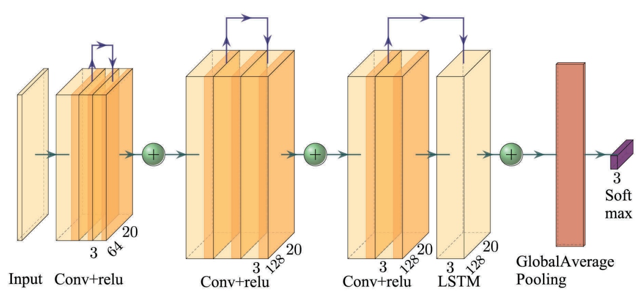

Fig. 4. Intent recognition network structure diagram.

occurrence of accidents). Due to the complex features and diverse lane-changing behaviors in such environments, the data generated by the GAN may not adequately reflect these features, leading to a decrease in the accuracy of the classification model. In addition, the model faces the same problem under extreme road or weather conditions (e.g. slippery, ice-covered roads). In the future, the adaptability of the model to diverse traffic environments can be enhanced by introducing methods such as self-supervised learning and adaptive learning.

In addition, the training set we use employs lane-changing trajectories that are screened for trajectories with universal lane-changing characteristics, and the vehicles do not produce round-trip behavior on the horizontal axis during lane-changing. However, in real-world scenarios, the behavior of vehicles is unpredictable, and the accuracy of intent recognition decreases for trajectories with such unpredictability. For the network to be able to predict the behavior of such trajectories, it has to take into account the trend of the trajectory over a shorter period of time, but this also reduces the robustness of the model. Intent recognition of unpredictable vehicle behavior in mixed traffic environments is difficult to achieve with a single model alone. For these complex and unpredictable driving behaviors, more diverse scene data and higher frequency trajectory sampling need to be considered when designing intent recognition models to capture more subtle trajectory changes. However, simply shortening the sampling period or focusing on short-term trajectory trends often leads to increased fluctuations in the model's prediction accuracy and reduces the model's ability to generalize across different scenarios. In mixed traffic environments, a combination of technical tools such as multi-model fusion, adaptive learning and scene awareness may be required to improve the model's adaptability and robustness under different complex driving behaviors.

4. Platoon Control Based on Intent Recognition

This section proposes a platoon control method based on the lane change intent recognition model introduced in Sec. 3. At each time step, the vertical spacing is adjusted based on the intent recognition module's assessment of surrounding vehicles' lane change intentions, aiming to prevent collisions with lane-changing vehicles. The lead vehicle prioritizes safe driving after receiving information about surrounding vehicles and their intentions. Meanwhile, the following vehicles in the platoon consider both the stability and safety of the platoon. The lead vehicle employs a control method based on intent recognition to switch control targets according to detected intentions. When surrounding vehicles exhibit a lane change intent, the lead vehicle ensures safe driving. In the absence of detected lane change intentions, it enables accurate and timely trajectory tracking. The remaining vehicles in the platoon use sliding mode control to maintain a safe distance between vehicles, ensuring the safety and stability of the platoon.

4.1. *Platoon control*

To simplify the model, only the longitudinal control of the platoon is considered. Assuming the vehicles follow a linear two-degree-of-freedom model, i.e. $\dot{x}_0(t) = v_0(t), \dot{v}_0(t) = a_0(t)$ and $\dot{a}_i(t) = -\frac{1}{\tau_i} a_i(t) + \frac{u_i(t)}{\tau_i m_i}$, where $m = 1820(\mathrm{kg})$. The state of the vehicle model is represented as $x^T = [x_i, v_i, a_i]$, where x_i, v_i, and a_i denote the longitudinal position, longitudinal velocity, and longitudinal acceleration of the ith vehicle, respectively. The time constant is denoted as $\tau = 0.28$, and the state space equation of the vehicle model is shown in Eq. (1).

In order to ensure the safe distance between platoon, the vehicle spacing error is defined as $e_i = x_{i-1} - x_i - \Delta_i$, and the safe distance $\Delta_i = l_i + q_i v_i + r_i a_i^2$, take $l_i = 10(\mathrm{m})$, and set the sliding mode surface as follows:

$$s_i = ce_i + \dot{e}_i. \tag{4}$$

Take the sliding mode approach rate:

$$\dot{s} = -\varepsilon \mathrm{sgn}(s) - ks. \tag{5}$$

Take the Lyapunov function:

$$V = \frac{1}{2} s^2. \tag{6}$$

Taking the derivative of V, we get

$$\dot{V} = s\dot{s} = -\varepsilon |s| - ks^2 < 0. \tag{7}$$

For any nonzero s, V is positive definite, $\dot{V}$ is negative definite, and as s approaches infinity, V also approaches infinity. Therefore, the system is globally asymptotically stable. Based on the system state space, we can obtain

$$\begin{aligned} \dot{s}_i &= c\dot{e}_i + \ddot{e} \\ &= c(v_{i-1} - v_i - q_i a_i - r_i v_i a_i) \\ &\quad + a_{i-1} - a_i - r_i a_i^2 - (q + r_i v_i)\left(-\frac{a_i}{\tau_i} + \frac{u_i}{\tau_i m_i}\right). \end{aligned} \tag{8}$$

Substituting the exponential approach rate into Eq. (5), at each sampling moment, the system input can be obtained as

$$\begin{aligned} &u_i(k+1) \\ &\quad = \frac{\tau_i m_i}{q + r_i v_i(k)} (\varepsilon \cdot \mathrm{sgn}(s) + ks + c(v_{i-1}(k) - v_i(k)) \\ &\qquad + r_i a_i(k)^2 + cq_i a_i(k) + cr_i v_i(k) a_i(k) + a_i(k) \\ &\qquad - a_{i-1}(k)) + m_i a_i(k). \end{aligned} \tag{9}$$

4.2. *Platoon control based on intent recognition*

Integrating the content from Sec. 3, the intention recognition results are introduced in addition to the single-vehicle model and the platoon controller. A controller is designed to enable the lead vehicle in the platoon to yield to vehicles merging into the same lane based on their lane-changing intentions. The simulation of vehicle lane-changing scenarios is conducted using the Prescan vehicle simulation software. The lead vehicle uses millimeter-wave radar to detect the position of surrounding vehicles as shown in Fig. 5.

In Fig. 5, the positive x-axis represents the vehicle's longitudinal direction, and the positive y-axis is to the left of the vehicle's travel direction. In the equations, ρ denotes the distance from the millimeter-wave radar to the measured vehicle, and φ represents the angle between the measured object and the x-axis.

Additionally, due to the scanning characteristics of the millimeter-wave radar, the output results may exhibit discontinuities and require filtering. First, the radar data are transformed from polar coordinates to Cartesian coordinates, and the relationship between target distance and relative velocity is given by

$$\begin{aligned} y &= \rho \cos \varphi, \\ x &= \rho \sin \varphi, \\ v_y &= \dot{\rho} \sin \varphi, \\ v_x &= \dot{\rho} \cos \varphi, \end{aligned} \tag{10}$$

where y, x, v_y and v_x represent the longitudinal relative distance, lateral relative distance, longitudinal relative velocity, and lateral relative velocity between the lead vehicle and surrounding vehicles, respectively.

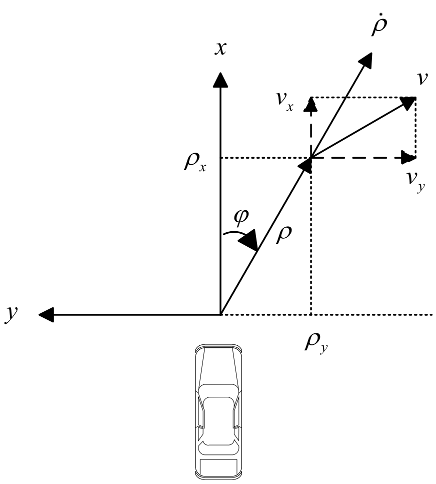

Fig. 5. Millimeter wave radar detection diagram.

Due to interference from external signals in real-world conditions, it is necessary to consider filtering the signals received by the millimeter-wave radar. The relationships among surrounding vehicles are as follows:

$$\begin{aligned} y_k &= y_{k-1} + \Delta_t v_{y,k-1} + \omega_y, \\ x_k &= x_{k-1} + \Delta_t v_{x,k-1} + \omega_x, \\ v_{y,k} &= v_{y,k} + \omega_{v_y}, \\ x_{x,k} &= x_{x,k} + \omega_{v_x}. \end{aligned} \tag{11}$$

The state variables and process noise are as shown in Eq. (12), where, the influence of input from surrounding vehicles is considered within the process noise:

$$\begin{aligned} X &= [x, y, v_x, v_y], \\ W &= [\omega_y, \omega_x, \omega_{v_y}, \omega_{v_y}]. \end{aligned} \tag{12}$$

Transforming the kinematic relationships into the form of state-space equations and applying the forward Euler method for discrete-time conversion, we obtain

$$\begin{aligned} X_k &= AX_{k-1} + W_k, \\ Z_k &= HX_k + V_k, \end{aligned} \tag{13}$$

where X_k represents the actual state at time k, $A = \begin{bmatrix} 1 & 0 & \Delta_t & 0 \\ 0 & 1 & 0 & \Delta_t \\ 0 & 0 & 1 & 0 \\ 0 & 0 & 0 & 1 \end{bmatrix}$, H is an identity matrix with the same dimensions as the state X_k, W_k is the process noise with zero mean and variance Q and V_k is the measurement noise with zero mean and variance R. According to the Kalman filter, the prior estimate at time k is

$$\hat{X}_{k^-} = A\hat{X}_{k-1}, \tag{14}$$

where $\hat{X}_{k-1}$ represents the posterior estimate at time $k-1$, and the prior error covariance matrix at time k is

$$P_{k^-} = AP_{k-1}A^T + Q, \tag{15}$$

where P_{k-1} represents the system error covariance matrix at time $k-1$. The Kalman gain is then computed as follows:

$$K_k = \frac{P_{k^-}H_k^T}{H_k P_{k^-} H_k^T + R}. \tag{16}$$

According to the Kalman gain, the posterior estimate at time k is

$$\hat{X}_k = \hat{X}_{k^-} + K_k(Z_k - H_k\hat{X}_{k^-}). \tag{17}$$

Finally, update the error covariance matrix:

$$P_k = (I - K_k H_k)P_{k^-}. \tag{18}$$

Through Kalman filtering, the actual position of the measured vehicle, combining the filtering result with the lead vehicle's own state, is represented as

$$\begin{aligned} y_s &= y_0 + y, \\ x_s &= x_0 + x, \\ v_{y,s} &= v_{y,0} + v_y, \\ v_{x,s} &= v_{x,0} + v_x, \end{aligned} \tag{19}$$

where y_s, x_s, $v_{y,s}$ and $v_{x,s}$ represent the longitudinal position, lateral position, longitudinal velocity, and lateral velocity of surrounding vehicles, respectively.

We input positional and velocity information of surrounding vehicles within the past 2 s, with a time interval of 0.1 s, into the intention recognition model. The model outputs probabilities for the vehicle's intentions, including changing lanes to the left or right and maintaining the current lane. Subsequently, in conjunction with the angle of the measured vehicle detected by the millimeter-wave radar, the intention to change lanes in or out is determined. The specific transitions for Left lane change (LC), Right lane change (RC) and Lane keep (LK) intentions are detailed in Table 1.

When there are no vehicles changing lanes into the current lane, the platoon proceeds along the planned trajectory. In speed control, considerations include tracking input while avoiding excessively large accelerations that may pose a risk to the vehicle. The speed of the lead vehicle is controlled using a PID control method, ensuring that the lead vehicle can track the trajectory speed. Let the velocity tracking error be defined as $e(k) = v_{\text{des}}(k) - v_i(k)$. For $\dot{a}_i(t) = -\frac{1}{\tau_i} a_i(t) + \frac{u_i(t)}{\tau_i m_i}$, taking the Laplace transform on both sides:

$$sA(s) = -\frac{1}{\tau_i} A(s) + \frac{1}{\tau_i m_i} U(s). \tag{20}$$

Then the open-loop transfer function of the system is

$$G_u(s) = \frac{A(s)}{U(s)} = \frac{1}{(s\tau_i + 1)m_i}. \tag{21}$$

According to the PID control principle, design the system input as

$$U(s) = \left(K_p + \frac{K_i}{s} + K_d s\right) E(s). \tag{22}$$

Table 1. Lane-changing intention.

Angle	LC	RC	LK
>0	Change out	Change in	lane keep
<0	Change in	Change out	lane keep

Assuming the reference input is $R(s)$, the closed-loop transfer function of the system is

$$\begin{aligned} G_r(S) &= \frac{A(s)}{R(s)} \\ &= \frac{\tau_i m_i s^2 + m_i s}{(\tau_i m_i + K_d)s^2 + (m_i + K_p)s + K_i}. \end{aligned} \tag{23}$$

Through a trial-and-error approach, the values are determined as $K_p = 20$, $K_i = 0.3$ and $K_d = 3.065$ for the PID controller of the lead vehicle's speed when there are no vehicles changing lanes into the current lane:

$$\begin{aligned} u_i(k) = K_p e_i(k) + K_i \sum_{j=0}^{k} e_i(j)\Delta t \\ + K_d \frac{e_i(k) - e_i(k-1)}{\Delta t}. \end{aligned} \tag{24}$$

When a lane-changing intention is detected in the surrounding vehicles, the longitudinal distance between the surrounding vehicle and the lead vehicle is given by $\Delta_x = x_s - x_0$, where the lead vehicle maintains a fixed safety distance $\Delta_s = 10(\text{m})$ with the lane-changing vehicle. Based on the intention recognition probability, different weights γ are assigned to the safety distance Δ_{env}. When $0.5 < P_I < 0.7$, the weight is $\gamma = 0.7$. When $0.7 < P_I < 0.9$, the weight is $\gamma = 0.85$. And when $0.9 < P_I$, the weight is $\gamma = 1$.

Define the spacing error between the lead vehicle and surrounding vehicles as $e_s = \Delta_x - \gamma\Delta_s$. Set the sliding surface as $s_s = ce_s + \dot{e}_s$, and use $\dot{s}_s = -\varepsilon \cdot \text{sgn}(s) - ks$ as the sliding mode approaching rate. Let $g = v_s(k-1) - v_0(k-1) - q_0 a_0(k-1) - r_0 v_0(k-1) a_0(k-1)$. At this point, the controller for the lead vehicle transforms to

$$\begin{aligned} u_0(k+1) = {} & \frac{\tau_0 m_0}{\gamma(k)(q + r_0 v_0(k))} (\varepsilon \cdot \text{sgn}(s) + ks \\ & + cg + \gamma(k)(a_s(k) - a_0(k) \\ & - r_0 a_0(k)^2)) + m_0 a_0(k), \end{aligned} \tag{25}$$

where, $a_s(k-1)$ represents the acceleration of surrounding vehicles at time step $k-1$, and $a_0(k-1)$ represents the acceleration of surrounding vehicles at time step $k-1$. When there are no lane-changing vehicles in the vicinity, i.e. when $P_I < 0.5$, the lead vehicle switches to PID control to achieve tracking of the reference speed.

5. Simulation

In this paper, we first give the analysis of the expansion results of TimeGAN on vehicle lane-changing data and compare the accuracy of the model when the expanded data and the original data are used as the training set, respectively. Second, we build the platoon vehicles and the surrounding vehicles changing into the scene in Prescan, import the trained model into Simulink, and illustrate the effectiveness of the method proposed in this paper through the joint simulation of Matlab/Simulink/Prescan.

5.1. *Simulation results of intention recognition algorithm*

The NGSIM I-80 and NGSIM US-101 datasets encompass diverse traffic scenarios. To gain a better understanding of vehicle lane-changing behavior, this paper initially conducts feature extraction and analysis on the NGSIM I-80 and NGSIM US-101 datasets. Key features of different lane-changing behaviors, including vehicle positions, velocities, and other information, are extracted from the datasets as input features for the network. These features serve as essential information foundations for subsequent intention recognition. Additionally, in the NGSIM dataset, the data points have a time interval of 0.1 s, but there are discontinuous frames. To ensure data continuity, this study employs interpolation to fill the gaps between discontinuous frames in the data.

In addition, the driving styles of vehicles are classified into short-term and long-term driving styles [30], with short-term driving styles reflecting a driver's tendency to make choices in different scenarios and long-term driving styles reflecting a driver's behavioral characteristics over a longer period of time. Driving style can be influenced by driver factors and external factors, but it is difficult to obtain accurate driver information about surrounding vehicles in a short period of time. Due to the strong uncertainty between driver factors and lane-changing intention, this paper selects network features through external environmental factors.

This paper defines the following rules to determine the actual intent of vehicle trajectories. First, define the starting point as the first point in the complete trajectory where the vehicle heading angle θ exceeds a specified threshold; subsequently, identify the ending point as the first point after the starting point where θ falls below another predetermined threshold. If there is a change in the lane label between the starting and ending points, all points in the trajectory between them are considered to indicate a lane-changing intent. A time window of 2 s is selected with a rolling interval of 0.2 s. Sub-trajectories are extracted starting 2 s before the starting point, and intent labels are added until the last sub-trajectory does not include any point between the starting and ending points.

If there is no change in the lane label between the starting and ending points in a complete trajectory, the trajectory is considered not to have a lane-changing intent. A time window of 2 s is chosen with a rolling interval of 1 s. Sub-trajectories are continuously extracted from the beginning of the complete trajectory, and intent labels are added. The original data are augmented using the TimeGAN algorithm, and the distribution of the generated data is visualized using Principal Component Analysis (PCA). The training results are shown in Figs. 6 and 7.

The results indicate that the generated data points closely match the distribution of the original data points on the PCA plot. The generated data points align with the direction and range of the principal components, consistent with the original data. TimeGAN successfully captures the statistical characteristics of the original data. On the PCA plot, the distribution range of the generated data points is extensive and not confined to a specific region of the original data. This suggests that the data generated by TimeGAN exhibit diversity, rather than merely replicating certain patterns from the original data.

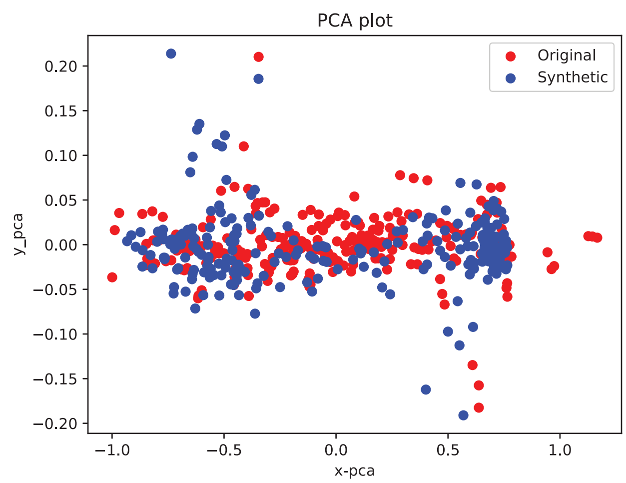

Fig. 6. Right lane change-generated data PCA result graph.

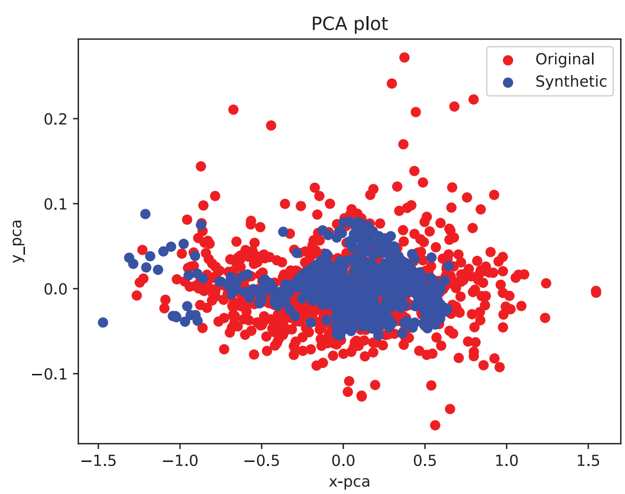

Fig. 7. Left lane change-generated data PCA result graph.

In addition, the proportion of explained variance for each principal component can be obtained through the proportion attribute of the PCA model. The following table demonstrates the proportions of the PCA principal components and their corresponding raw features for various intentions, with the numbers in front of the parentheses representing the features of the raw data to which the principal component corresponds, and the numerical value in the parentheses representing the proportion of variance explained for that principal component (PC).

In Table 2, it is observed that the principal components of the generated data and the principal components of the original data show similarity in terms of features, and all the principal components of the generated data are consistent with the features corresponding to the principal components of the original data. Moreover, the principal components of the generated data are similar to the principal components of the original data in terms of direction and proportion, and the maximum difference in proportion is 0.110, which reflects the effectiveness of the generative algorithm in maintaining consistency with the original data.

Besides, we compare the accuracy of data generated by three algorithms, GAN, DoppelGANger [31], and TimeGAN, in the recognition algorithm. The quantitative analysis of the three methods is shown in Table 3, through which it can be seen that both GAN and DoppelGANger are less accurate than TimeGAN in the vehicle lane-changing dataset.

After feature extraction, trajectory completion, and data augmentation, the augmented lane-changing dataset is fed into the intention recognition network. The LSTM network is capable of capturing the temporal features of vehicle lane-changing behavior, aiding in a more accurate identification of lane-changing intent. The learning rate is set to $\alpha = 0.1$, and the training is conducted for 100 epochs. The accuracy of the recognition model with different GAN algorithms expanding the data through iterative training is shown in Fig. 8, and the accuracy of the recognition model without the GAN algorithm is shown in Fig. 9.

Table 2. Proportion of principal components.

Principal component	LC	RC	LK
PC 1 (raw)	2(0.853)	3(0.976)	3(0.968)
PC 2 (raw)	3(0.781)	2(0.913)	1(0.996)
PC 1 (generated)	2(0.778)	3(0.896)	3(0.913)
PC 2 (generated)	3(0.762)	2(0.851)	1(0.886)

Table 3. Accuracy of different GAN models.

GAN algorithm	TimeGAN	DoppelGANger	GAN
Accuracy	0.9354	0.9268	0.9240

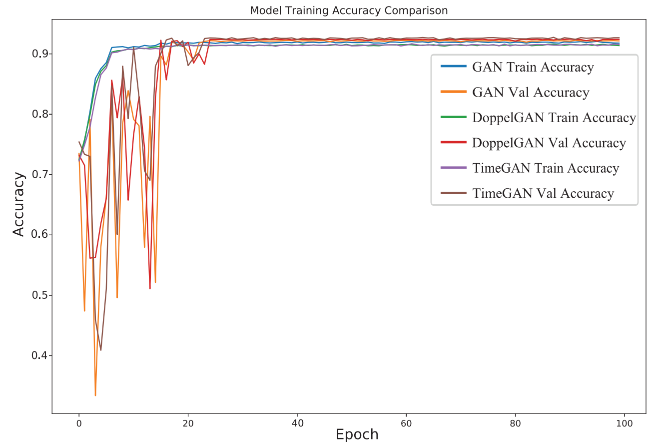

Fig. 8. Accuracy of different GAN models.

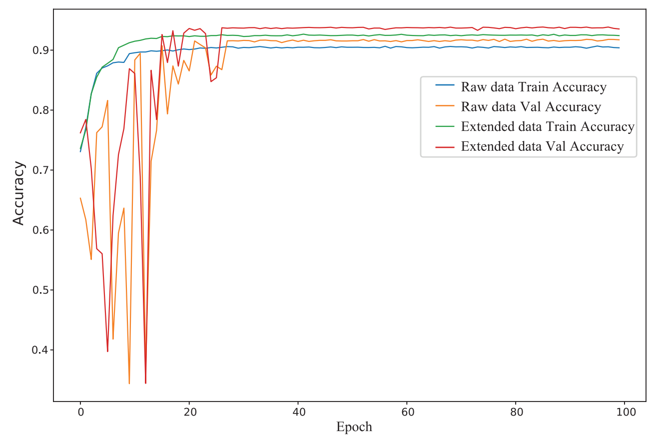

Fig. 9. Extended data training result graph.

The training accuracy for the augmented data is 0.9354, while the training accuracy for the original data is 0.9173. Through augmentation of the original data, the training accuracy of the intention recognition network is improved by 0.0181. Experimental results indicate that the proposed lane-changing intent recognition method based on data generation algorithms achieves a certain performance improvement in scenarios involving lane-changing vehicles. This provides reliable support for the platoon to effectively respond to lane-changing behaviors of other vehicles in real-world traffic.

5.2. *Simulation results of vehicle platoon control based on intent recognition*

This paper employs joint simulation using Matlab/Simulink/Prescan. To emphasize the impact of the intention recognition model on the platoon, the platoon is appropriately simplified. It consists of 5 vehicles, and there is a lane-changing vehicle ahead of the platoon. The total length of the road is 120 m, and the lane width is 3.2 m. At 3 s, the lane-changing vehicle changes into the lane where the platoon is located. In Prescan, the lead vehicle's millimeter-wave radar scan wavelength is set to 100 m, and the beam is set to 5, capable of detecting targets within a range of -22.5° to 22.5° in front of the vehicle.

The platoon proceeds in its lane, and surrounding vehicles change lanes into the same lane. The millimeter-wave radar is utilized to detect information about the surrounding vehicles, and intention recognition is performed. Platoon control is then based on the results of intention recognition. The method proposed in this paper is shown in Fig. 10.

To simulate the complex scenario in the real environment, we set up four surrounding vehicles (SV), in which SV2 and SV4 will change lanes, and SV1 and SV3 always keep their original lanes. During the whole lane change process, SV4's lane change will affect the platoon vehicles, and we set SV2 to interfere with the intention recognition module. The experimental results show that our intention recognition models are all able to recognize both SV2 and SV4 and can react to SV4.

For the platoon head vehicle, the vehicles in the left and right lanes closest to it and the front vehicle in this lane have the greatest influence on it. In the experimental process, SV2 is far away from the head vehicle and will be occluded by SV4, and its subsequent intention recognition is not meaningful. And the target that is far away will have a vacancy because of the occlusion of the trajectory of other vehicles, which has an impact on the intention recognition. Therefore, when two vehicles change lanes to this lane at the same time, first judge the distance of the lane-changing vehicle from the head vehicle, and then control it according to the nearest surrounding vehicles from the head vehicle.

In the simulation scenario built in Prescan, we use four intent recognition modules to simultaneously identify the intent of the surrounding vehicles. Among them, SV2 and SV4 are able to recognize the existence of the intention to change lanes, and the target id recognized by the radar changes when SV2 is occluded by SV4. In order to ensure the validity of the input data of the intention recognition module, we added target id detection before the recognition module to avoid the sudden change of data caused by occlusion. In addition, we also tested the performance gap between one intent recognition module and four intent recognition modules, and the results show that one module takes 0.03873 s, while four modules take 0.04651 s to predict simultaneously. The detection results of the intention recognition model are illustrated in Fig. 11.

At 4.4 s, the probability of SV4 being detected by the intent recognition model is 66.118%. The lead vehicle adjusts its platoon spacing according to the lane change probability obtained by the intent recognition module. The simulation results are shown in Figs. 12 and 14.

The desired speed is maintained by the platoon vehicles according to the control method designed in Sec. 4. The leader vehicle of the platoon, according to the intention recognition module, first carries out deceleration to keep a safe distance from the lane-changing vehicle, and at 5.2 s, the intention recognition module considers that the lane-changing of the surrounding vehicles is completed, and the controller controls the leader vehicle to carry out acceleration to reach the preset speed. The platoon vehicles then maintain a safe distance between the platoon according to the slip mode control. The simulation results of surrounding vehicles changing in from different directions are shown in Fig. 12.

The simulation results of the ideal and actual spacing between vehicles in the platoon when surrounding vehicles are approaching from different directions are shown in Fig. 13.

At 4.0 s, surrounding vehicles initiate lane-changing. The lead vehicle detects a significant lane-changing intent in the surrounding vehicles within 0.2 s and initiates deceleration.

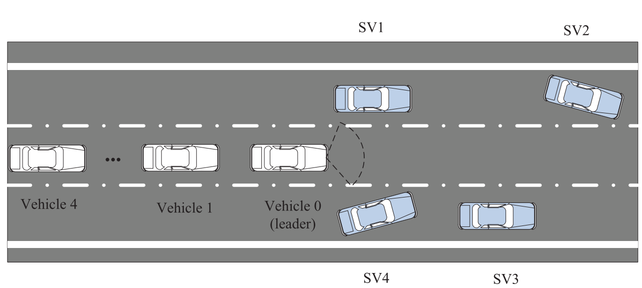

Fig. 10. Vehicle platoon simulation scenario.

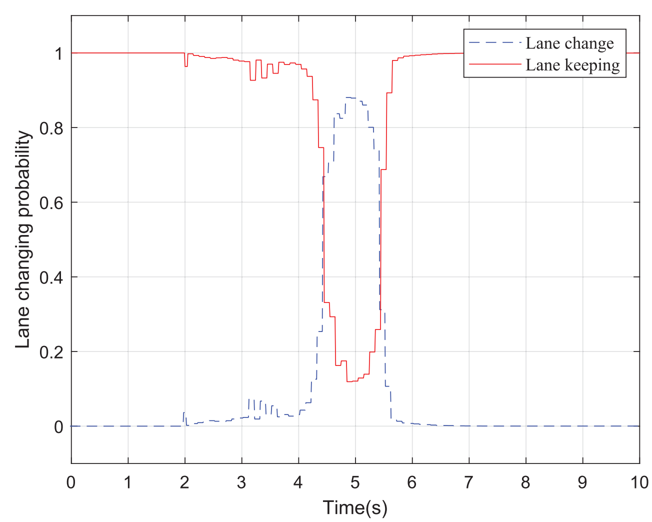

Fig. 11. Lane change probability.

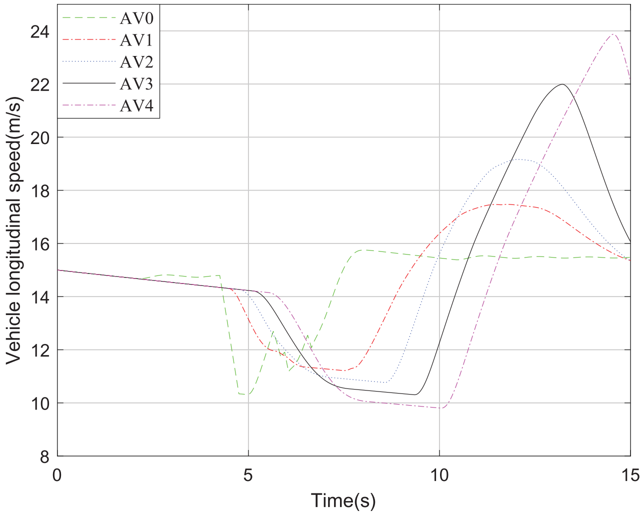

Fig. 12. Platoon speed profile.

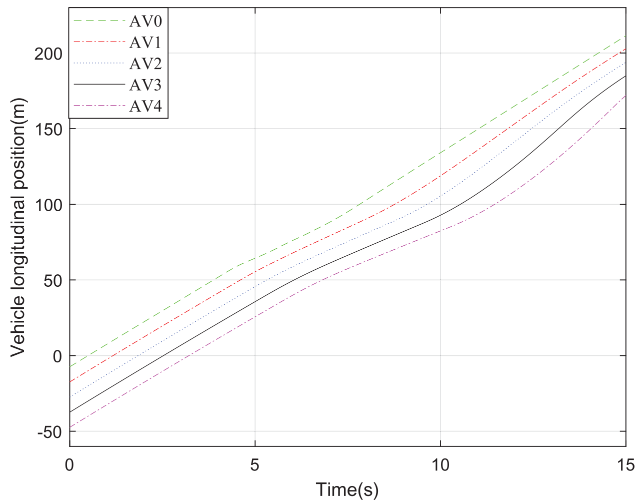

Fig. 13. Platoon distance plot.

Simultaneously, the following vehicle decelerates to maintain the spacing within the platoon. After the completion of the lane-changing process, the lead vehicle continues to keep a safe distance from the lane-changing vehicle until the lane-changing intent dissipates.

In addition, the work [32] also employs the NGSIM dataset for vehicle lane change intention recognition and the SVM algorithm to predict the lane change intention of the target vehicle. In the vehicle lane changing dataset extracted in this paper, the cross-validation accuracy is 0.9084 and the test accuracy is 0.8993. In the simulation scenario constructed at the beginning of this paper, the recognition results of the algorithm are shown

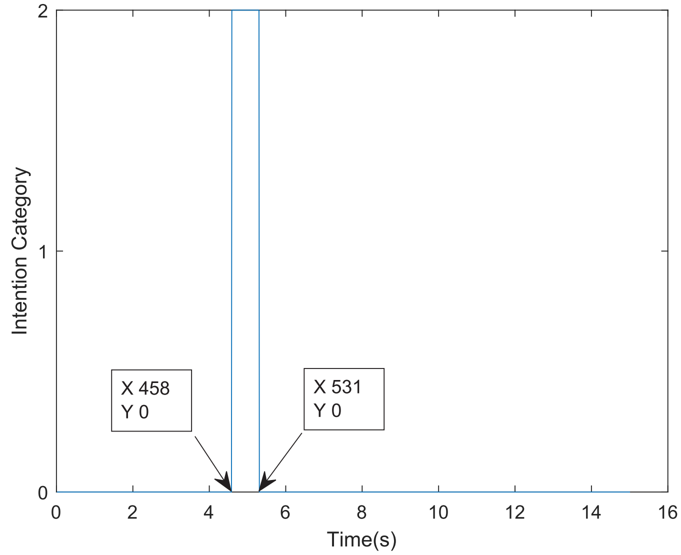

Fig. 14. SVM algorithm intent recognition results.

in Fig. 14. Where "0" represents right turn intention, "1" represents lane keeping intention and "2" represents left turn intention.

The SVM algorithm recognizes that the vehicle makes a lane change in 4.58 s, while the GAN-LSTM algorithm designed in this paper recognizes that the vehicle makes a lane change in 4.37 s. The algorithm in this paper can recognize the target vehicle's intention to change lanes earlier, providing more control reaction time for the controlled vehicle and increasing the safety and comfort of the vehicle.

6. Conclusion

This paper primarily investigates the combination of deep learning algorithms and control methods to detect lane-changing intentions of surrounding vehicles in a platoon. A controller is designed to decelerate the lead vehicle to facilitate avoidance of surrounding vehicles. The other vehicles in the platoon maintain an appropriate safe distance based on sliding mode control and the lead vehicle's speed, ensuring the stable operation of the platoon. The proposed method can detect lane-changing intentions of surrounding vehicles in the early stages and implement platoon avoidance control. The recognition model achieves an accuracy of 0.9354 when provided with a 2-second history trajectory as input. In simulated scenarios, the intention recognition probability exceeds 50%, and the deviation from the actual lane-changing point is 0.4 s, enhancing platoon safety under specific conditions.

Acknowledgments

This work was supported by the National Key Research and Development Plan under Grant 2022YFE0100100.

ORCID

Yige Ren https://orcid.org/0009-0002-3447-7694
Kang Song https://orcid.org/0000-0002-7548-2214
Jin Guo https://orcid.org/0000-0003-3863-8811
Yanlong Zhao https://orcid.org/0000-0003-0131-3597

References

[1] Y. Liu, J. Liu, Z. He, Z. Li, Q. Zhang and Z. Ding, A survey of multi-agent systems on distributed formation control, *Unmanned Syst.* **12**(1) (2023) 1–14, doi: 10.1142/S2301385024500274.

[2] E. S. Steven, PATH at 20-history and major milestones, *IEEE Trans. Intell. Transp. Syst.* **8**(4) (2007) 584–592, doi: 10.1109/TITS.2007.903052.

[3] L. Li and P. Li, Analysis of driver's steering behavior for lane change prediction, in *Proc. — Int. Conf. Intell. Human-Mach. Syst. Cybern. (IHMSC)*, Hangzhou, China, 2019, pp. 71–75, doi: 10.1109/IHMSC.2019.10112.

[4] S. Lee, M. Q. Khan and M. N. Husen, Continuous car driving intent detection using structural pattern recognition, *IEEE Trans. Intell. Transp. Syst.* **22**(2) (2020) 1001–1013, doi: 10.1109/TITS.2019.2961928.

[5] X. Ji, C. Fei, X. He, Y. Liu and Y. Liu, Driving intention recognition and vehicle trajectory prediction based on LSTM network, *China J. Highw. Transp.* **32**(6) (2019) 34–42.

[6] D. J. Phillips, T. A. Wheeler and M. J. Kochenderfer, Generalizable intention prediction of human drivers at intersections, in *IEEE Intell. Veh. Symp. Proc.*, Los Angeles, CA, USA, 2017, pp. 71–75, doi: 10.1109/IVS.2017.7995948.

[7] Q. Shangguan, T. Fu, J. Wang, S. Fang and L. Fu, A proactive lane-changing risk prediction framework considering driving intention recognition and different lane-changing patterns, *Accid. Anal. Prev.* **164** (2022) 106500, doi: 10.1016/j.aap.2021.106500.

[8] R. Yuan, M. Abdel-Aty, X. Gu, O. Zheng and Q. Xiang, A unified modeling framework for lane change intention recognition and vehicle status prediction, *Phys. A Stat. Mech. Appl.* **632** (2023) 129332, doi: 10.1016/j.physa.2023.129332.

[9] D. He, M. Zhao and Z. Wang, Vehicle driving intent recognition based on enhanced bidirectional long short-term memory network, *J. Artif. Intell. Pract.* **6** (2023) 20–27, doi: 10.23977/jaip.2023.060504.

[10] S. Li, L. Zhang, D. Yu and Y. Tian, Driving lane change intent recognition based on vehicle exterior environment variables, in *Chinese Control Conf. (CCC)*, Wuhan, China, 2018, pp. 9315–9319, doi: 10.23919/ChiCC.2018.8483804.

[11] Y. Guo, H. Zhang, C. Wang, Q. Sun and W. Li, Driver lane change intention recognition in the connected environment, *Phys. A Stat. Mech. Appl.* **575** (2021) 126057, doi: 10.1016/j.physa.2021.126057.

[12] F. Dong, X. Zhao and Y. H. Chen, Optimal longitudinal control for vehicular platoon systems: Adaptiveness, determinacy, and fuzzy, *IEEE Trans. Fuzzy Syst.* **29**(4) (2020) 889–903.

[13] S. Y. Han, Y. H. Chen, L. Wang and A. Abraham, Decentralized longitudinal tracking control for cooperative adaptive cruise control systems in a platoon, in *Proc. — IEEE Int. Conf. Syst., Man, Cybern. (SMC)*, Manchester, UK, 2013, pp. 2013–2018, doi: 10.1109/SMC.2013.345.

[14] L. Jiang, Y. Xie, N. G. Evans, X. Wen, T. Li and D. Chen, Reinforcement learning based cooperative longitudinal control for reducing traffic oscillations and improving platoon stability, *Transp. Res. Part C Emerg. Technol.* **141** (2022) 103744, doi: 10.1016/j.trc.2022.103744.

[15] H. B. Jond and A. Yildiz, Connected and automated vehicle platoon formation control via differential games, *IET Intell. Transp. Syst.* **17**(2) (2023) 312–326, doi: 10.1049/itr2.12260.

[16] Y. Zhang, Y. Wen, F. Li and Y. Chen, Distributed observer-based formation tracking control of multi-agent systems with multiple targets of unknown periodic inputs, *Unmanned Syst.* **7**(1) (2019) 15–23, doi: 10.1142/S2301385019400028.

[17] V. Turri, B. Besselink and K. H. Johansson, Cooperative look-ahead control for fuel-efficient and safe heavy-duty vehicle platooning, *IEEE Trans. Control Syst. Technol.* **25**(1) (2016) 12–28, doi: 10.1109/TCST.2016.2542044.

[18] W. B. Dunbar and D. S. Caveney, Distributed receding horizon control of vehicle platoons: Stability and string stability, *IEEE Trans. Autom. Control* **57**(3) (2011) 620–633, doi: 10.1109/TAC.2011.2159651.

[19] Y. Zheng, S. E. Li, K. Li, F. Borrelli and J. K. Hedrick, Distributed model predictive control for heterogeneous vehicle platoons under unidirectional topologies, *IEEE Trans. Control Syst. Technol.* **25**(3) (2016) 899–910, doi: 10.1109/TCST.2016.2594588.

[20] D. Li, S. Wu, J. Lu, Z. Zang, Z. Li and Z. Tang, Platoon control of unmanned tracked vehicles based on distributed model prediction, in *2021 China Automation Congress (CAC)*, Beijing, China, 2021, pp. 3549–3554.

[21] Z. Zang, J. Song, Y. Lu, X. Zhang, Y. Tan, Z. Ju, H. Dong, Y. Li and J. Gong, A unified framework integrating trajectory planning and motion optimization based on spatio-temporal safety corridor for multiple AGVs, *IEEE Trans. Intell. Veh.* **9**(1) (2023) 1217–1228, doi: 10.1109/TIV.2023.3285911.

[22] Z. Zang, J. Gong, Z. Li, J. Song, H. Liu, C. Gong, X. Zhang and Y. Li, Formation trajectory tracking control of UTVs: A coupling multi-objective iterative distributed model predictive control approach, *IEEE Trans. Intell. Veh.* **8**(3) (2022) 2222–2232, doi: 10.1109/TIV.2022.3229773.

[23] K. Hou, F. Zheng, X. Liu and Z. Fan, Cooperative vehicle platoon control considering longitudinal and lane-changing dynamics, *Transp. A Transp. Sci.* **20**(3) (2024) 2182143, doi: 10.1080/23249935.2023.2182143.

[24] S. Lei, J. Li, Z. Wei, Kai Yang, E. Hashemi and H. Wang, Longitudinal and lateral control methods from single vehicle to autonomous platoon, *Green. Energy. Intell. Transp.* **2**(2) (2023) 100066, doi: 10.1016/j.geits.2023.100066.

[25] F. Zhao, Y. Liu, J. Wang and L. Wang, Distributed model predictive longitudinal control for a connected autonomous vehicle platoon with dynamic information flow topology, *Actuators* **10**(9) (2021) 204, doi: 10.3390/act10090204.

[26] D. Huang, S. Li, Z. Zhang, Y. Liu and B. Mi, Design and analysis of longitudinal controller for the platoon with time-varying delay, *IEEE Trans. Intell. Transp. Syst.* **23**(12) (2022) 23628–23639, doi: 10.1109/TITS.2022.3200026.

[27] Y. Li, S. Zhang, L. Huang and G. Huang, Nonlinear longitudinal co-operative control of heterogeneous connected vehicle platoon considering car-following interactions and communication delay, *Transp. B Transp. Dyn.* **11**(1) (2023) 1687–1706, doi: 10.1080/21680566.2023.2241643.

[28] I. Goodfellow, J. Pouget-Abadie, M. Mirza, B. Xu, D. Warde-Farley, S. Ozair, A. Courville and Y. Bengio, Generative adversarial networks, *Commun. ACM* **63**(11) (2020) 139–144, doi: 10.1145/3422622.

[29] J. Yoon, D. Jarrett and M. Van der Schaar, Time-series generative adversarial networks, in *Advances in Neural Information Processing Systems*, Vol. 32 (Curran Associates, 2019), pp. 5508–5518.

[30] H. Chu, H. Zhuang, W. Wang, X. Na, L. Guo, J. Zhang, B. Gao and H. Chen, A review of driving style recognition methods from short-term and long-term perspectives, *IEEE Trans. Intell. Veh.* **8**(11) (2023) 4599–4612, doi: 10.1109/TIV.2023.3279425.

[31] Z. Lin, A. Jain, C. Wang, G. Fanti and V. Sekar, Using GANs for sharing networked time series data: Challenges, initial promise, and open questions, in *Proc. ACM Internet Measurement Conf. (IMC '20)*, New York, USA, 2020, pp. 464–483, doi: 10.1145/3419394.3423643.

[32] J. Yao, G. Chen and Z. Gao, Target vehicle selection algorithm for adaptive cruise control based on lane-changing intention of preceding vehicle, *Chin. J. Mech. Eng.* **34**(1) (2021) 135, doi: 10.1186/s10033-021-00650-8.